
Forearm Motion Simulation during Pro-Supination for Improved Surgical Planning

Technical Report

Authors :

Noura Hamze

Fabio Carrillo

Markus Walzhöni

Philipp Färnstahl

Matthias Harders

This work is supported by the Swiss National Science Foundation, under grant number 325230L_163308, and the Austrian Science Fund FWF, under grant number I 2545-N31.

1 Introduction

Forearm osteotomy is an orthopedic surgical procedure which aims to heal bone deformities and related complex pathologies. Biomechanical simulations have already been proposed to improve existing computer-assisted preoperative planning for orthopedic surgery. The aim of such simulations is providing dynamic simulations that allow for a comprehensive analysis of complex pathologies, as well as a larger range of possible intervention strategies. Despite the fact that accurate models of soft tissue behavior are key elements in medical simulation systems, most preoperative methods are currently limited to simple bone-based procedures, not taking into account the influence of soft tissue at all, or rely on over-simplified behaviour.

In this report, we present a modular numerical simulation framework which enables the inclusion of various behaviour models for complex soft tissue in the context of preoperative planning. We show a pro-supination simulation as a proof of concept.

2 Overview of the System

An outline of our system is illustrated in Figure 1. It consists of two main units :

- An atlas-based pipeline for landmark transfer which is fed into a modelling unit, the latter is responsible to generate a geometric model for the simulation scene. These components have been presented in [4].
- A simulation unit (the front-end), which allows performing pro-supination simulations for the forearm ; it is highly modular and permits the use of several behaviour laws. This unit will be detailed in the present report.

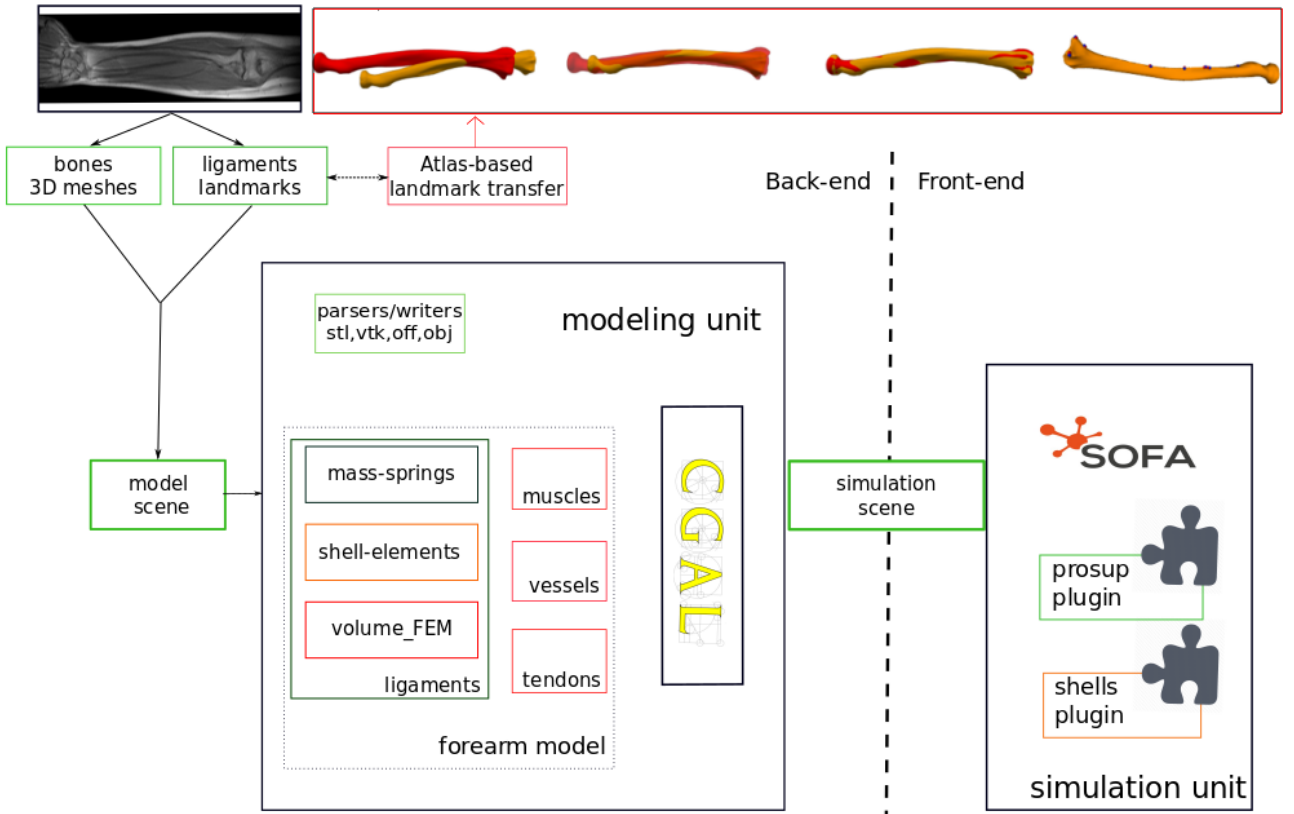


FIGURE 1 – Outline

3 Materials and Methods

3.1 Description of the kinematic motion

Pro-supination is the rotational motion of the forearm in which the radius bone rotates around the ulna, allowing the human body to flip the palm either face up (in supination) or face down (in pronation). Several elements contribute to the stability of the distal radioulnar joint during this motion. In particular, the interosseous membrane (IOM), the radioulnar ligaments (RULs) and the triangular disc which is a fibrocartilage structure connecting the radius and ulna at the surface of the wrist. In the following, we explain the necessary elements to perform a numerical simulation which is capable of reproducing the kinematic prescribed motion.

3.2 Numerical simulation

The forearm complex with its bones and ligamentous soft tissues are regarded as rigid and deformable objects which are subject to the laws of continuum mechanics. One numerical method to solve the governing equations of motion is the finite element method (FEM). A dynamic system can be represented by :

$$\mathbf{M}\Delta\mathbf{v} = h(\mathbf{f}(\mathbf{x}, t))$$

where \mathbf{x} is the vector of degrees of freedom, $\Delta\mathbf{v} = \mathbf{v}(t_0 + h) - \mathbf{v}(t_0)$, h is the time step, \mathbf{M} the mass matrix, and $\mathbf{f}(\mathbf{x}, t)$ a function representing all the internal and external forces, which act on the system. A solution for the linear system obtained from the ordinary differential equations (ODEs) is found following an implicit Euler scheme as presented in [1].

The simulation has to follow certain restrictions on the way its particles are permitted to move ; for instance, the ulna should remain fixed during the motion, the radius rotates around a specific axis, the ligaments should stay connected to the bones, etc. Constrained dynamics [5] is a convenient approach to address such kind of restrictions/constraints. A constraint problem can be expressed as

$$\left(\mathbf{M} + dt \frac{\partial \mathbf{f}}{\partial \dot{\mathbf{x}}} + dt^2 \frac{\partial \mathbf{f}}{\partial \mathbf{x}} \right) \Delta\mathbf{v} = -dt(\mathbf{f} + dt \frac{\partial \mathbf{f}}{\partial \mathbf{x}} \mathbf{v} - \mathbf{H}^T \boldsymbol{\lambda}).$$

The previous equation can be rewritten as

$$\mathbf{A} \Delta\mathbf{v} = \mathbf{b} + dt \mathbf{H}^T \boldsymbol{\lambda},$$

where $\mathbf{H}^T \boldsymbol{\lambda}$ is the vector of constraint forces, with matrix \mathbf{H} containing the constraint directions, and $\boldsymbol{\lambda}$ are the Lagrange multipliers.

We differentiate between two types of constraints in our system : projective and bilateral.

- Projective constraints are used in our simulation to fix the ulna, and to restrict the motion of the radius to a rotational component without any translational movement. When applied on a certain vertex, the solver will project a constant velocity, which will attach the vertex to its initial position
- Bilateral constraints are used to handle the ligament-bone interactions involved in the simulation.

A constraint law is assigned which depends of the relative positions of the interacting objects.

$$\Phi(\mathbf{x}_1, \mathbf{x}_2, \dots) = 0$$

To solve the dynamics of two constrained objects, we use a Lagrange multipliers approach and a single linearization by time step. In the constrained system presented above, the constraint matrix \mathbf{H} can be written as :

$$\mathbf{H}(\mathbf{x}) = \left[\frac{\partial \Phi}{\partial \mathbf{x}} \right]$$

For two interacting objects (illustration in Fig. 2), the complete constrained system therefore corresponds to :

$$\begin{aligned} \mathbf{A}_1 \Delta\mathbf{v}_1 &= \mathbf{b}_1 + dt \mathbf{H}_1^T \boldsymbol{\lambda} \\ \mathbf{A}_2 \Delta\mathbf{v}_2 &= \mathbf{b}_2 + dt \mathbf{H}_2^T \boldsymbol{\lambda} \end{aligned}$$

The resolution of the problem is done in two steps. Firstly, the interacting objects are solved independently by setting $\boldsymbol{\lambda} = 0$ and the so called free motions $\Delta\mathbf{v}_1^{free}$ and $\Delta\mathbf{v}_2^{free}$ are obtained for each object. After that, the constraints are taken into account by setting $\mathbf{b}_1 = \mathbf{b}_2 = 0$, and a corrective motion is computed and applied to the free motion in order to retrieve the final resolution.

$$\begin{aligned} \mathbf{x}_1 &= \mathbf{x}_1^{free} + dt \cdot \Delta\mathbf{v}_1^{cor} \\ \mathbf{x}_2 &= \mathbf{x}_2^{free} + dt \cdot \Delta\mathbf{v}_2^{cor}, \end{aligned}$$

with $\Delta\mathbf{v}_1^{cor} = \mathbf{A}_1^{-1} \mathbf{H}_1^T \boldsymbol{\lambda}$ and $\Delta\mathbf{v}_2^{cor} = \mathbf{A}_2^{-1} \mathbf{H}_2^T \boldsymbol{\lambda}$. The simulations have been implemented in the Open Simulation Framework Architecture (SOFA)[3].

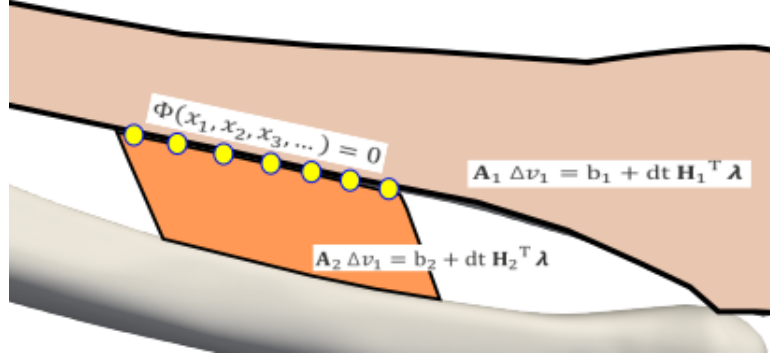


FIGURE 2 – Illustration of bilateral constraints between a bone and a ligament.

3.3 Material behavior law

Different constitutive laws have been tested for the three types of anatomical structures within the simulations.

3.3.0.1 Cartilages and Triangular Fibrocartilage Discus (TFC) : All cartilage structures have been modeled as meshes composed of volume tetrahedral elements; and various hyperelastic material laws, including Mooney Rivlin and St. Venant Kirchhoff have been employed.

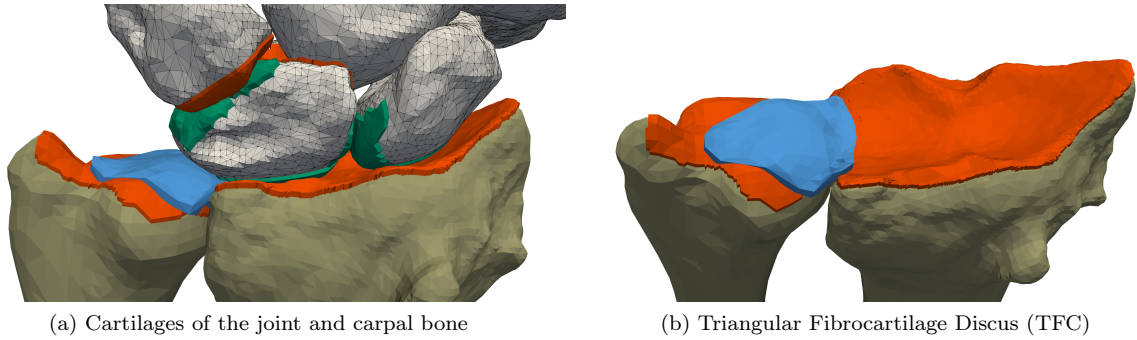


FIGURE 3 – Cartilages and TFC are modeled as volume tetrahedron elements

3.3.0.2 Forearm ligaments : Several models have been proposed to model the ligaments. Firstly, a simplified mass-spring model has been implemented. Later, we used more accurate geometric models to obtain more accurate shapes. For the radio-ulnar ligaments, which are part of the Triangular fibrocartilage complex (TFCC), 3D volume meshes were more suitable to approximate their shapes; and we relied on a Neo-Hookean behaviour law with a co-rotational FE formulation for the strains to allow larger displacement and better wrapping.

As for the interosseous membrane (IOM), we followed a different model; the use of shell theory allows to model deformations of thin anatomical structures like ligaments. In addition, it allows plausible collision handling and wrapping during bending, thanks to a recursive-subdivision collision detection approach, proposed in [2].

3.3.0.3 Bony structures : The bones are modeled as geometrical 3D triangular surface meshes with rigid properties.

3.4 Collision handling

The collision detection is implemented in two phases. A broad phase, in which collision between the bounding boxes of the colliding objects is tested, and a narrow phase, in which a classical intersection method based on the minimal proximity intersection is used. In the latter, a contact is created when collision elements (geometric primitives of triangles, lines, and vertices) are close to each other. Once a contact is detected between two objects, a response is created.

The response to the collision has been customized using two rules; in the first one, a repulsion force based on penalties is applied when a collision between two bones or between a ligament and a bone is detected. In the second rule, a friction force is generated when collision happens with a cartilage.

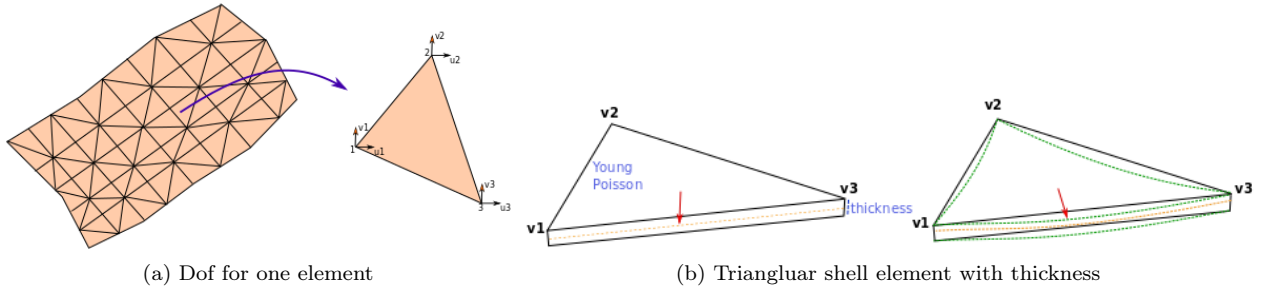


FIGURE 4 – A ligament surface modeled as triangular shell elements

Given the complex model of the forearm, a collision algorithm in which all possible intersections between the primitives will be tested is computationally expensive. Therefore, collision groups have been defined in order to accelerate the simulation. The idea is to avoid unnecessary tests by regrouping the model elements which are likely to collide in a separate group. For example, the radioulnar ligaments do not collide with the IOM and thus, they are placed in different groups. Finally, the process is considerably accelerated by using optimized collision surfaces, instead of the complete original mesh of the bones. The collision surfaces are subsets, which are manually delineated from coarser meshes and located at the possible collision regions. Examples are the violet and pink patches in Fig. 5

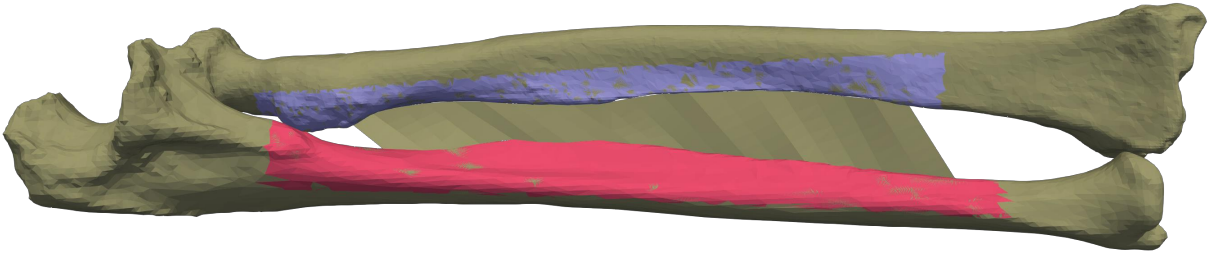


FIGURE 5 – Collision surfaces between the IOM and bones (purple for the radius and pink for the ulna).

4 Experiments and Simulation Scenarios

Based on the presented methods, a pro-supination simulation has been implemented and tested in various configurations, where the IOM is modeled either as a single band or separated into different ligamentous structures. Selected simulation videos are available on the project's YouTube channel. In both scenarios, an increasing torque is applied on the distal side of the radius, causing its rotation around a predefined rotational axis, which passes through the proximal end of the radius and the center of the distal side of the ulna. The ulna remains fixed during the motion, via a fixation constraint applied on its center of mass; and the radius is allowed to rotate without a translation via a translational constraint applied on its proximal side.

In healthy forearms, the range of motion (ROM) from full supination to full pronation equals about 180 degrees; but it can be limited in case of injuries. In our simulations, the ROM is governed by many factors, mainly the stiffness of the ligaments and their anatomy. The simulations show that varying the elasticity parameter of the IOM when modeled as a single, wide band leads to different ROMs. Fig. 6 illustrates examples for three simulations, each corresponding to a different value of Young's modulus for the IOM : 25 kPa, 37.5 kPa and 50 kPa, for the blue, yellow, and pink ROM, respectively.

A validation approach based on ex-vivo studies has been proposed and partially implemented. The idea is to set up a cadaver study in which a configuration allows to perform passive pro-supination thanks to a mounting device with a torque applicator. Fig 7 illustrates the experiment. During the motion, a number of MR images should be acquired at different steps of the motion which correspond to predefined angles of rotation. The bones of the radius and ulna should be segmented at intermediate intervals and be used further as a ground truth to which the positions of the bones in the numerical simulations should be compared.

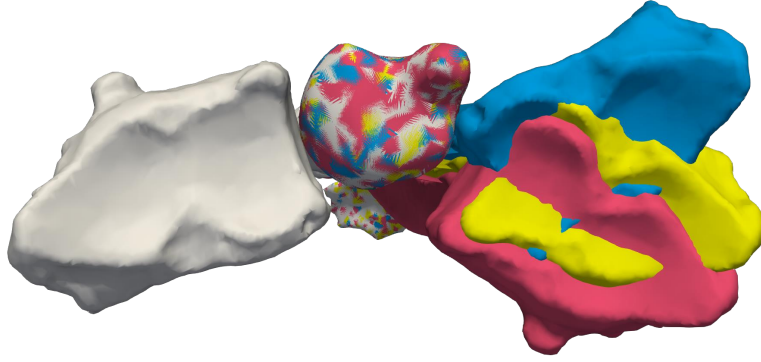


FIGURE 6 – Lateral view - Influence of Young's moduli of the IOM on the ROM (25 kPa for pink 37.5 kPa for yellow and 50 kPa for blue).

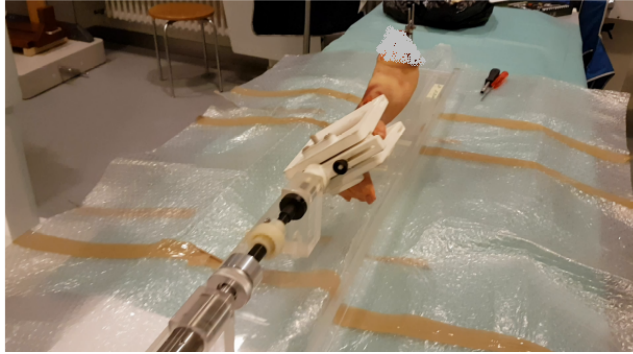


FIGURE 7 – A forearm specimen is mounted on the device to perform pro-supination motion.

5 Discussion

In this report, we presented a finite element method approach based on constrained dynamics for the simulation of forearm pro-supination. The work had been carried out in the context of preoperative surgical planning. Two main challenges could be identified : Firstly, it was not possible to obtain accurate anatomical shapes using medical segmentation techniques ; we had to rely on geometric modelling approach as an alternative, which has its limitations. Secondly, the validation of such complex numerical simulations is not trivial. A few concerns also exist regarding the outlined validation :

1. In the experimental study, the hand of the specimen has been left intact, and the torque is applied on the meta-carpal bones, while it is applied directly on the radius in our simulations. In order to reproduce the same setting. All the carpal bones and ligaments, as well as the TFCC anatomy should be included in the simulation. This adds further variability in the simulation, due to the inaccuracy in both their geometric and behaviour models.
2. The assumption that the ulna is fixed during the motion is not accurate. In the experiment, the forearm is fixed at the upper part and the elbow joint is left intact. A slight movement of the ulna could still be observed.
3. It is difficult to obtain patient-specific biomechanical properties of the hand ligaments ; in the literature large variability has been encountered, including a sub-study implemented during this project.
4. The simulation suffers from typical errors in discretization and numerical approximation ; in the collision detection, the accuracy of the constitutive laws, or the sensitivity of the solver parameters.

Nevertheless, a first step towards numerical simulation of pro-supination, with the complex anatomy of the forearm has been undertaken. The proposed methods allow to perform simulations with different constitutive laws for the soft tissue. To the best of our knowledge, our simulations go beyond the majority available in the current state of the art. Still, there is considerable room remaining for investigation, validation, and improvement.

Références

- [1] David Baraff and Andrew Witkin. Large steps in cloth simulation. In *Proceedings of the 25th annual conference on Computer graphics and interactive techniques - SIGGRAPH 98*. ACM Press, 1998.
- [2] Olivier Comas, Christian Duriez, and Stéphane Cotin. Shell model for reconstruction and real-time simulation of thin anatomical structures. In Tianzi Jiang, Nassir Navab, Josien P. W. Pluim, and Max A. Viergever, editors, *Medical Image Computing and Computer-Assisted Intervention – MICCAI 2010*, pages 371–379. Springer Berlin Heidelberg, 2010.
- [3] François Faure, Christian Duriez, Hervé Delingette, Jérémie Allard, Benjamin Gilles, Stéphanie Marchesseau, Hugo Talbot, Hadrien Courtecuisse, Guillaume Bousquet, Igor Peterlik, and Stéphane Cotin. SOFA : A Multi-Model Framework for Interactive Physical Simulation. In Yohan Payan, editor, *Soft Tissue Biomechanical Modeling for Computer Assisted Surgery*, volume 11 of *Studies in Mechanobiology, Tissue Engineering and Biomaterials*, pages 283–321. Springer, June 2012.
- [4] Noura Hamze, Lukas Nocker, Nikolaus Rauch, Markus Walzthöni, Fabio Carrillo, Philipp Färnstahl, and Matthias Harders. Automatic modelling of human musculoskeletal ligaments – framework overview and model quality evaluation. *arXiv e-prints*, 2020.
- [5] Andrew Witkin. Physically based modeling : Principles and practice constrained dynamics, 1997.